13 Feb 2012

Influence of Solid-Phase Wall Boundary Condition on CFD Simulation of Spouted Beds

Xingying Lan

Chunming Xu

Jinsen Gao

Muthanna H. Al-Dahhan
Missouri University of Science and Technology, aldahhanm@mst.edu

Recommended Citation

X. Lan et al., "Influence of Solid-Phase Wall Boundary Condition on CFD Simulation of Spouted Beds," *Chemical Engineering Science*, vol. 69, no. 1, pp. 419 - 430, Elsevier, Feb 2012.
The definitive version is available at https://doi.org/10.1016/j.ces.2011.10.064

Chemical Engineering Science 69 (2012) 419–430

Contents lists available at SciVerse ScienceDirect

Chemical Engineering Science

journal homepage: www.elsevier.com/locate/ces

Influence of solid-phase wall boundary condition on CFD simulation of spouted beds

Xingying Lan [a], Chunming Xu [a], Jinsen Gao [a], Muthanna Al-Dahhan [b,*]

[a] State Key Laboratory of Heavy Oil Processing, China University of Petroleum, Beijing 102249, China
[b] Chemical & Biological Engineering, Missouri University of Science and Technology, Rolla, MO 65401, USA

ARTICLE INFO

Article history:
Received 12 May 2011
Received in revised form
9 September 2011
Accepted 28 October 2011
Available online 12 November 2011

Keywords:
Spouted beds
Numerical simulation
Boundary condition
Hydrodynamics
Specularity coefficient
Particle-wall restitution coefficient

ABSTRACT

The influence of solid-phase wall boundary condition in terms of specularity coefficient and particle–wall restitution coefficient on the flow behavior of spouted beds was investigated using two-fluid model approach in the computational fluid dynamics software FLUENT 6.3. Parametric studies of specularity coefficient and particle–wall restitution coefficient were performed to evaluate their effects on the flow hydrodynamics in terms of fountain height, spout diameter, pressure drop, local voidage and particles velocity. The numerical predictions were compared with available experimental data in the literatures to obtain the suitable values of specularity coefficient and particle–wall restitution coefficient for spouted beds. The simulated results show that the solid-phase wall boundary condition plays an important role in CFD modeling of spouted beds. The specularity coefficient has a pronounced effect on the spouting behavior and a small specularity coefficient (0.05) can give good predictions, while the particle–wall restitution coefficient is not critical for the holistic flow characteristics.

1. Introduction

Spouted beds are widely used in various industrial processes, such as drying, coating, granulation, pyrolysis and gasification, due to their efficiency in contacting gases and coarser particles. Knowledge about gas and particles hydrodynamics in spouted beds is important for the design and scale-up of spouted beds. During the past five decades, much of spouted bed research has been carried out with various techniques such as piezoelectirc probe, capacitance probe, cine-photography, γ-ray, β-ray absorption, radiocative tracer and fiber optic probe. Recently, computational fluid dynamics (CFD) is becoming an alternative approach to investigate the complex hydrodynamics in spouted beds. The two-fluid model (TFM) and the discrete element method (DEM) are generally adopted in the CFD modeling of spouted beds. From the point of view of computation, the TFM approach is much more commonly used in the practical spouting flow modeling.

Huilin et al. (2004) incorporated hydrodynamic modeling with a kinetic–frictional constitutive model of solids to simulate the gas–solids flow in spouted beds. Du et al. (2006a, 2006b) investigated the influences of drag coefficient correlations, frictional stress, maximum packing limit and restitution coefficient on the CFD simulation of spouted beds based on TFM approach. Bettega et al. (2009b, 2009c) used Eulerian–Eulerian 3D modeling to analyze the influence of the flat wall on the solids behavior inside a semi-cylindrical spouted bed by comparing numerical results with experimental data. Bettega et al. (2009a) also verified that CFD simulation could be used to evaluate the similitude method for spouted beds scale-up. Duarte et al. (2009) simulated the dynamic behavior in conical and conical–cylindrical spouted beds. Gryczka et al. (2009) characterized the hydrodynamics of a prismatic spouted bed apparatus by applying TFM approach. Shuyan et al. (2009) discussed the impact of frictional stresses on the gas–solids flow by using an Eulerian–Eulerian two-fluid model with the kinetic–frictional constitutive model of particles, and then simulated the flow behavior of gas and particles in spouted beds with a draft tube (Shuyan et al., 2010b) and a porous draft tube (Shuyan et al., 2010a), respectively. The works mentioned above suggest that the CFD modeling based on TFM approach is able to predict the complex hydrodynamics in different types of spouted beds.

Spouted beds can be roughly divided into three different regions, each with its own specific flow behavior: the spout, the annulus and the fountain (Mathur and Epstein, 1974). The solids volume fractions vary from almost zero to nearly the maximum packing limit, and particles in different regions are present in different states. The inter-particle collisions are subject to significantly different energy losses. In addition, solid particles are enduring strong frictional contact with multiple neighbors due to the high volume fraction in the annulus, and therefore the

* Corresponding author. Tel.: +1 573 341 4416.
E-mail address: aldahhanm@mst.edu (M. Al-Dahhan).

0009-2509/$ - see front matter © 2011 Elsevier Ltd. All rights reserved.
doi:10.1016/j.ces.2011.10.064

frictional stress cannot be neglected. When using the TFM approach to simulate the gas–solids spouted beds, different phases are mathematically treated as interpenetrating continua, and the conservation equations for each of two phases are derived to obtain a set of equations that have similar structure for each phase. The success of TFM depends on the proper description of all possible intra- and inter-phase interactions, such as gas–solids interactions, collision and frictional interactions between particles, and interactions between particles and wall. The reported works in the literature have investigated the effect of gas–solids interactions in terms of drag correlations and the collision and frictional interactions between particles on the spouting flow, and furthermore have given some useful suggestions (Du et al., 2006a, 2006b). Unfortunately, less effort in the literature has been given to the influence of interactions between particles and wall on the flow behavior of spouted beds.

It was reported that correct wall boundary conditions for gas and solids phases were critical for proper prediction of the hydrodynamics in laboratory and small-scale columns (Li et al., 2010a). A no-slip boundary condition is commonly used for gas phase, however, there has been no consistency on what kind of wall boundary conditions should be used to represent the interactions between wall and solids. Johnson and Jackson (1987) wall boundary condition is generally applied in the CFD simulations of gas–solids flow. This wall boundary condition involves two important parameters, the specularity coefficient, φ, and the particle–wall restitution coefficient, e_w. The former specifies the shear condition at the walls, and the latter describes the dissipation of the solids kinetic energy with the wall by collisions. For $\varphi=0$, a free-slip boundary condition without frictional effect of particles on the wall is used, while when $\varphi=1$, a no-slip boundary condition with frictional effect of particles on the wall is employed. Unfortunately, these two coefficients are difficult to measure, and their experimental values are rarely reported. Different values have been found to be used in the open literatures. Benyahia et al. (2005) suggested that the specularity coefficient may be set in relatively dense flow conditions where particles collisions were dominant. For the dilute turbulent flow of glass beads ($d_p=70$ μm, $\rho_s=2500$ kg m^{-3}) in a pipe, using a free-slip boundary condition (close to a small or no friction limit) compared better with experimental data. Benyahia et al. (2007) also suggested that a low specularity coefficient value was essential to predict the core-annulus flow regime in the isothermal flow of glass beads ($d_p=0.12$ mm, $\rho_s=2400$ kg m^{-3}) in a vertical channel. Almuttahar and Taghipour (2008) found that for the flow of fluid catalytic cracking (FCC) particles in a high density circulating fluidized bed, using a smaller specularity coefficient wall boundary condition, a higher solids volume fraction near the wall was predicted which was in a better agreement with the experimental data. However no-slip and relatively high slip boundary conditions underestimated the solids concentration. Wang et al. (2009) modeled the hydrodynamics of a high flux circulating fluidized bed with Geldart group A particles, and reported that a small specularity coefficient could give well predictions, and the particle–wall restitution coefficient was not critical for the holistic distribution trends of solids volume fraction and solids velocity. Li et al. (2010b) recommended that the solid-phase wall boundary condition needs to be specified with great care when the gas mixing in the bubbling bed with glass beads ($d_p=0.155$ mm, $\rho_s=2420$ kg m^{-3}) with free-slip, partial-slip and no-slip wall boundary conditions was modeled. Substantial differences in the extent of gas downwards transport at the wall were found. Zhang and Yu (2002) reported that the slugging behavior of fluidized beds with large particles ($d_p=0.5$ mm, $\rho_s=2660$ kg m^{-3}) heavily depends on the wall boundary conditions, and different conditions resulted in different types of slugs.

For the CFD simulation of spouted beds, no-slip, partial-slip and free-slip wall boundary conditions have been used in the literature. Among them, the no-slip boundary condition was widely used (Du et al., 2006a, 2010b; Zhonghua and Mujumdar, 2008; Bettega et al., 2009a, 2009c; Duarte et al., 2009; Gryczka et al., 2009; Shuyan et al., 2009, 2010a, 2010b; Dan et al., 2010), the particle-slip boundary condition was used by Bettega et al. (2009b), and the free-slip boundary condition was only used by Wang et al. (2006). These studies just used these wall boundary conditions without giving the reason. Moreover, no systemic study on the influence of wall boundary conditions on the spouting behavior has been reported. Therefore, the present work will investigate the flow dynamics of spouted beds at different solid-phase wall boundary conditions, with particular interest in evaluating the effect of the specularity coefficient and particle–wall restitution coefficient on the spouting behavior. The numerical predictions are compared with the available experimental data in the literature to obtain the suitable values of specularity coefficient and particle–wall restitution coefficient for the CFD simulation of spouted beds.

2. CFD model for spouted beds

The two-fluid model (TFM) is applied to simulate the complicated gas–solids flow in spouted beds. By TFM approach, the gas–solids two phases are treated mathematically as continuous and fully interpenetrating. Generalized Navier–Stokes equations are used for the interacting continua. To close the governing equations, the constitutive relations are needed. Because the solid phase is treated as continuous, it has similar properties to a continuous fluid. Using the kinetic theory of granular flows (Ding and Gidaspow, 1990), the viscous forces and the pressure of solids phase can be described as a function of the granular temperature (Lun et al., 1984). The stress of solids phase due to frictional interactions between particles is represented by the Schaeffer (1987) model. The governing equations and constitutive relations for spouted beds are shown in Table 1.

In spouted beds, the gases and particles in the spout region rise at high velocities, while particles move slowly downwards in the annulus region between the spout and the wall. In the spout and fountain region, the influences of gas turbulent fluctuations on overall gas–solids flow behavior exist. However, due to the nature of the flow structure in spouted beds, the turbulence would not be the dominant factor in determining the solids flow characteristics. There has been no consistency on whether turbulent fluctuation effects should be considered and which turbulent model is the most suitable for CFD simulation of spouted beds. Du (2006) applied the dispersed turbulence model and the per-phase turbulence model to simulate the flow in spouted beds. The results showed that the dispersed turbulence model could predict reasonable trends of spouting flow, while the per-phase turbulence model overestimated the particles turbulent fluctuations and could not predict the spouting flow trends. Hence, in the present work, the dispersed turbulence model has been adopted, where turbulence predictions for gas phase are obtained by the standard k–ε model supplemented with extra terms that include the inter-phase turbulent momentum transfer. The equations of k–ε turbulence model are shown in Table 1. Tchen theory (Hinze, 1975) of particles dispersion by homogeneous turbulence has been used to describe the turbulence quantities for particles phase. The related expressions have been reported in Du et al. (2006a).

The interaction of gas and solids phases can be represented by a gas–solids drag coefficient. Du et al. (2006a) investigated the influence of different drag models on the hydrodynamics of

Table 1
Governing equations and constitutive relations for spouted beds.

Governing equations

1. *Continuity equations of gas and solids phase*

$$\frac{\partial}{\partial t}(\alpha_g\rho_g)+\nabla\cdot(\alpha_g\rho_g v_g)=0 \quad (T1-1)$$

$$\frac{\partial}{\partial t}(\alpha_s\rho_s)+\nabla\cdot(\alpha_s\rho_s v_s)=0 \quad (T1-2)$$

$$\alpha_g+\alpha_s=1 \quad (T1-3)$$

2. *Momentum equations of gas and solids phase*

$$\frac{\partial}{\partial t}(\alpha_g\rho_g v_g)+\nabla\cdot(\alpha_g\rho_g v_g v_g)=-\alpha_g\nabla P+\nabla\cdot\bar{\bar{\tau}}_g+\beta(v_s-v_g)+\alpha_g\rho_g g \quad (T1-4)$$

$$\frac{\partial}{\partial t}(\alpha_s\rho_s v_s)+\nabla\cdot(\alpha_s\rho_s v_s v_s)=-\alpha_s\nabla P_s+\nabla\cdot\bar{\bar{\tau}}_s+\beta(v_g-v_s)+\alpha_s\rho_s g \quad (T1-5)$$

where

$$\bar{\bar{\tau}}_g=\alpha_g\mu_g\left\{\left[\nabla v_g+(\nabla v_g)^{\mathrm{T}}\right]-\tfrac{2}{3}\nabla\cdot v_g\bar{\bar{I}}\right\} \quad (T1-6)$$

$$\bar{\bar{\tau}}_s=\alpha_s\mu_s\left[\nabla v_s+(\nabla v_s)^{\mathrm{T}}\right]+(\alpha_s\lambda_s-\tfrac{2}{3}\alpha_s\mu_s)\nabla\cdot v_s\bar{\bar{I}} \quad (T1-7)$$

3. *Granular temperature equation (Ding and Gidaspow, 1990)*

$$\frac{3}{2}\left[\frac{\partial}{\partial t}(\rho_s\alpha_s\Theta_s)+\nabla\cdot(\alpha_s\rho_s v_s\Theta_s)\right]=(-\nabla P_s\bar{\bar{I}}+\bar{\bar{\tau}}_s):\nabla v_s+\nabla\cdot(\Gamma_{\Theta s}\nabla\Theta_s)-\gamma_{\Theta s}-3\beta\Theta_s \quad (T1-8)$$

Constitutive equations

1. *Solids pressure*

$$P_s=\alpha_s\rho_s\Theta_s+2\rho_s(1+e_{ss})\alpha_s^2 g_{0,ss}\Theta_s \quad (T1-9)$$

2. *Solids shear viscosity*

$$\mu_s=\mu_{s,col}+\mu_{s,kin}+\mu_{s,fr} \quad (T1-10)$$

3. *Collisional viscosity(Gidaspow et al., 1992)*

$$\mu_{s,col}=\frac{4}{5}\alpha_s^2\rho_s d_s g_{0,ss}(1+e_{ss})\sqrt{\frac{\Theta_s}{\pi}} \quad (T1-11)$$

4. *Kinetic viscosity(Gidaspow et al., 1992)*

$$\mu_{s,kin}=\frac{10\rho_s d_s\sqrt{\pi\Theta_s}}{96(1+e_{ss})g_{0,ss}}\left[1+\frac{4}{5}g_{0,ss}\alpha_s(1+e_{ss})\right]^2 \quad (T1-12)$$

5. *Frictional viscosity(Schaeffer, 1987)*

$$\mu_{s,fr}=\frac{P_s\sin\phi}{2\sqrt{I_{2D}}} \quad (T1-13)$$

6. *Solids bulk viscosity (Lun et al., 1984)*

$$\lambda_s=\frac{4}{3}\alpha_s\rho_s d_s g_{0,ss}(1+e_{ss})\sqrt{\frac{\Theta_s}{\pi}} \quad (T1-14)$$

7. *Diffusion coefficient of granular energy (Gidaspow et al., 1992)*

$$\Gamma_{\Theta s}=\frac{150\rho_s d_s\sqrt{\pi\Theta_s}}{384(1+e_{ss})g_{0,ss}}\left[1+\frac{6}{5}\alpha_s g_{0,ss}(1+e_{ss})\right]^2+2\alpha_s^2\rho_s d_s g_{0,ss}(1+e_{ss})\sqrt{\frac{\Theta_s}{\pi}} \quad (T1-15)$$

8. *Collisional energy dissipation (Lun et al., 1984)*

$$\gamma_{\Theta s}=\frac{12(1-e_{ss}^2)g_{0,ss}}{d_s\sqrt{\pi}}\rho_s\alpha_s^2\Theta_s^{3/2} \quad (T1-16)$$

9. *Radial distribution function*

$$g_{0,ss}=\left[1-\left(\frac{\alpha_s}{\alpha_{s,max}}\right)^{1/3}\right]^{-1} \quad (T1-17)$$

10. *Gas viscosity*

$$\mu_g=\mu_{l,g}+\mu_{t,g},\quad \mu_{t,g}=C_\mu\alpha_g\rho_g\frac{k_g^2}{\varepsilon_g} \quad (T1-18)$$

11. *Turbulent kinetic energy equation*

$$\frac{\partial}{\partial t}(\alpha_g\rho_g k_g)+\nabla\cdot(\alpha_g\rho_g v_g k_g)=\nabla\cdot\left(\alpha_g\frac{\mu_{t,g}}{\sigma_k}k_g\right)+\alpha_g G_{k,g}-\alpha_g\rho_g\varepsilon_g+\alpha_g\rho_g\Pi_{k,g} \quad (T1-19)$$

12. *Turbulent kinetic energy dissipation rate equation*

$$\frac{\partial}{\partial t}(\alpha_g\rho_g\varepsilon_g)+\nabla\cdot(\alpha_g\rho_g v_g\varepsilon_g)=\nabla\cdot\left(\alpha_g\frac{\mu_{t,g}}{\sigma_\varepsilon}\varepsilon_g\right)+\alpha_g\frac{\varepsilon_g}{k_g}(C_{1\varepsilon}G_{k,g}-C_{2\varepsilon}\rho_g\varepsilon_g)+\alpha_g\rho_g\Pi_{\varepsilon,g} \quad (T1-20)$$

where

$$G_{k,g}=\mu_{t,g}(\nabla v_g+(\nabla v_g)^{\mathrm{T}}):\nabla v_g \quad (T1-21)$$

$C_\mu=0.09$, $C_{1\varepsilon}=1.44$, $C_{2\varepsilon}=1.92$, $\sigma_k=1$, $\sigma_\varepsilon=1.3$

13. *Gas–solid drag coefficient (Gidaspow et al., 1992)*

$$\beta=150\frac{\alpha_s^2\mu_g}{\alpha_g d_s^2}+1.75\frac{\alpha_s\rho_g|v_g-v_s|}{d_s},\quad \alpha_g<0.8 \quad (T1-22)$$

$$\beta=\frac{3}{4}C_D\frac{\alpha_s\alpha_g\rho_g|v_g-v_s|}{d_s}\alpha_g^{-2.65},\quad \alpha_g\geq 0.8 \quad (T1-23)$$

$$C_D=\begin{cases}\frac{24}{\alpha_g Re_s}(1+0.15(\alpha_g Re_s)^{0.687}) & (Re_s<1000)\\ 0.44 & (Re_s\geq 1000)\end{cases} \quad (T1-24)$$

$$\mathrm{Re}_s=\frac{\rho_g d_s|v_g-v_s|}{\mu_g} \quad (T1-25)$$

spouted beds, and concluded that the Gidaspow model (1992) gave the best agreement with experimental data. Other CFD simulations on spouted beds (Huilin et al., 2004; Wang et al. 2006; Zhonghua and Mujumdar, 2008; Bettega et al., 2009a; Shuyan et al., 2009) also demonstrated that the Gidaspow model could reasonably describe the gas–solids exchange coefficient. Hence, the Gidaspow model has been applied, and its expressions are also summarized in Table 1.

3. Simulation conditions and numerical solution method

3.1. Simulation conditions

The simulation conditions are based on the experimental work of He et al. (1994a, 1994b). In their experiments, a cylindrical plexiglas column of inside diameter 152 mm and height 1.4 m with a 60° conical base was tested. Closely sized glass beads with a mean diameter of 1.41 mm and density of 2503 kg m^{-3} were used as the particles. The spouting fluid was air at room temperature. The static bed height was 0.325 m. The geometry of the spouted bed simulated by CFD is shown in Fig. 1. The hydrodynamics of particles velocity and voidage were measured by the fiber optic probe.

3.2. Numerical solution method

The simulations of spouted beds have been carried out with the CFD package FLUENT 6.3. The set of governing equations mentioned in Section 2 have been solved by a finite control volume technique. The Phase Coupled SIMPLE algorithm, which is an extension of the SIMPLE algorithm for multiphase flow, has been used for the pressure–velocity coupling and correction. The momentum, volume fraction and turbulence equations have been discretized by a first-order upwind scheme.

Peirano et al. (2001) and Cammarata et al. (2003) suggested that two-dimensional (2D) CFD simulation would be appropriate when the flow by nature was or closed to two dimensional. For spouted beds, the variations of parameters in the tangential direction are negligible compared to the variations in the axial and radial directions. Therefore, 2D simulation has been used in this work to simulate spouted beds. 2D axial symmetry has been assumed. The dimensions of the computational domain in axial and radial directions are the same as those of the actual spouted bed. Grids have been created in a CAD program GAMBIT 2.4 and imported into FLUENT 6.3. The grids of the spouted bed simulated are shown in Fig. 2. A transient simulation has been adopted, using a very small time step of 0.0001 s with about 20 iterations per time step. A convergence criterion of 10^{-3} for each scaled residual component has been specified for the relative error between two successive iterations.

3.3. Initial and boundary conditions

Appropriate initial and boundary conditions of velocities, pressure and granular temperature are crucial for solving the equations listed in Table 1. The simulations start from a static bed. Particles are lying in the spouted bed with a maximum packing limit and the static bed height is equal to the fixed bed height of the experiment. The velocities of gas and solids phases are set to be zero.

At the inlet, the uniform distribution is assumed for velocity components, kinetic energy of turbulence and energy dissipation rate of gas phase. Gas is injected only in the axial direction, and

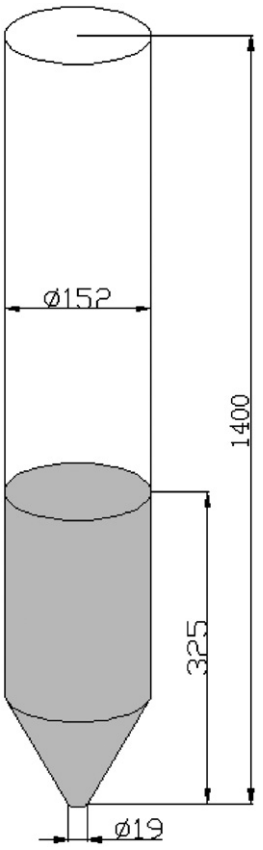

Fig. 1. The geometry of the spouted bed simulated.

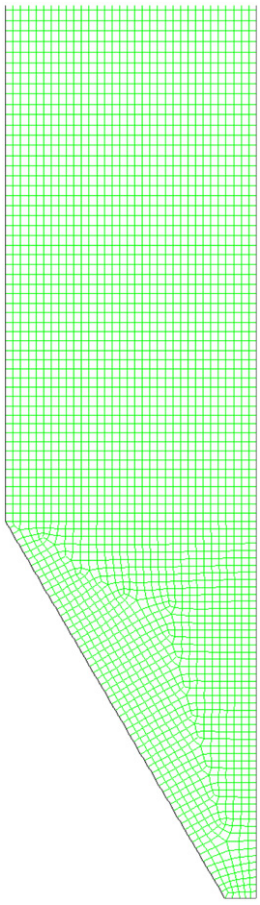

Fig. 2. The grids of the spouted bed simulated.

solids velocity is zero. The turbulent kinetic energy of gas phase is $k_g = 1.5(v_g I)^2$, where I is the turbulent intensity and is set as 10%. The turbulent dissipation rate of gas phase is $\varepsilon_g = C_\mu^{3/4}(k_g^{1.5}/l)$, where $l = 0.07D_h$. At the outlet, the pressure is set at an ambient atmosphere. At the axis of spouted bed, the velocity gradients for two phases and the granular temperature gradient of particles along the radial direction are assumed to be zero.

At the wall, the gas tangential and normal velocities are set to be zero. The normal velocity of particles is also set at zero. The Johnson and Jackson (1987) wall boundary condition is applied for the tangential velocity and granular temperature of solids phase at the wall. As expressed in Eqs. (1)–(3), the slip velocity between particles and the wall can be obtained by equating the tangential force exerted on the boundary and the particles shear stress close to the wall. Similarly, the granular temperature at the wall is obtained by equating the granular temperature flux at the wall to the inelastic dissipation of energy, and to the generation of granular energy due to slip at the wall region

$$v_{s,w} = -\frac{6\mu_s\alpha_{s,\max}}{\sqrt{3\Theta}\pi\varphi\rho_s\alpha_s g_{0,ss}}\frac{\partial v_{s,w}}{\partial n} \tag{1}$$

$$\Theta_w = -\frac{k_s\Theta}{\gamma_w}\frac{\partial\Theta_w}{\partial n} + \frac{\sqrt{3}\pi\varphi\rho_s\alpha_s v_{s,slip}^2 g_{0,ss}\Theta^{3/2}}{6\alpha_{s,\max}\gamma_w} \tag{2}$$

$$\gamma_w = \frac{\sqrt{3}\pi(1-e_w^2)\rho_s\alpha_s g_{0,ss}\Theta^{3/2}}{4\alpha_{s,\max}} \tag{3}$$

where φ is the specularity coefficient and e_w is the particle–wall restitution coefficient. The two coefficients are difficult to measure, and different values have been used in the open literatures on CFD simulation of gas–particles flow systems without a clear explanation of their choices. To evaluate their impacts on the flow behavior in spouted beds and obtain suitable values, different specularity coefficients and particle–wall restitution coefficients have been investigated in the present work. Five specularity coefficient values (φ=0, 0.01, 0.05, 0.1, 0.2 and 1) and three particle–wall restitution coefficient values (e_w=0.8, 0.9 and 0.99) have been used. Conditions and parameters for the numerical simulation of spouted beds are summarized in Table 2.

Table 2
Conditions and parameters for numerical simulations.

Item	Value
Gas density, kg m^{-3}	1.21
Gas viscosity, Pa s	1.81×10^{-5}
Particle diameter, mm	1.41
Particle density, kg m^{-3}	2503
Minimum spouting velocity, m s^{-1}	0.54
Static bed height, m	0.325
Superficial gas velocity, m s^{-1}	0.648
Sphericity of particles	1
Internal friction angle of particles	28
Loose packed voidage	0.412
Particle–particle restitution coefficient	0.9
Specularity coefficient	0, 0.01, 0.05, 0.2, 1
Particle–wall restitution coefficient	0.8, 0.9, 0.99
Grid resolution	36×186

4. Results and discussion

4.1. Grid independence study

The grid independence is first examined by comparing the simulation results using three grid sizes. The spout diameter and fountain height are important characteristic parameters, which

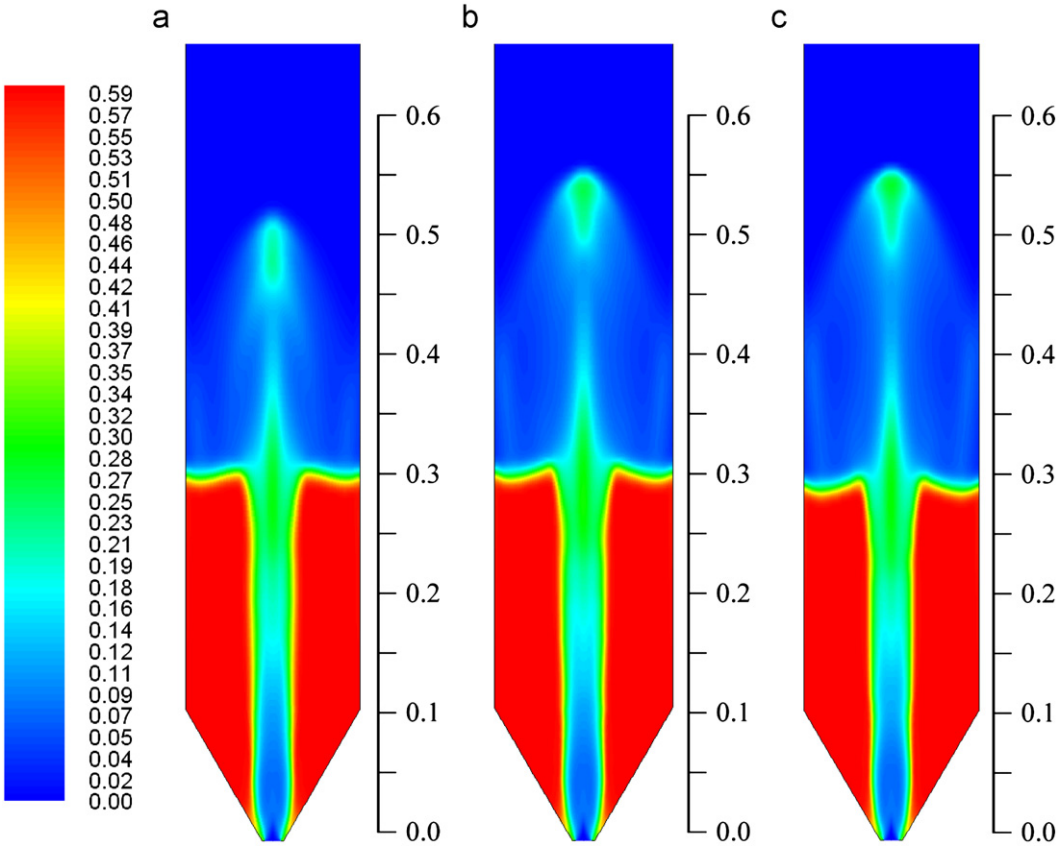

Fig. 3. Predicted solids volume fraction distribution for different grid resolutions. (a) 26×135, (b) 36×186, (c) 42×216.

can be used to determine how well numerical models capture the hydrodynamic behavior of spouted beds. As shown in Fig. 3, the predicted spout diameters are almost identical for three grids, and the predicted fountain height using medium grid resolution (36×186) are close to the height using finer grid resolution (42×216), but higher than the height using coarse grid resolution (26×135). Nearly grid-independent results can be obtained using the medium grid resolution in the current study. Thus, as a compromise between accuracy and computational cost, the following simulations are performed based on using medium grid resolution (36×186).

4.2. Effect of specularity coefficient

Fig. 4 shows the simulated solids volume fraction distribution in spouted beds using different φ. The typical flow pattern of spouted beds including three regions, the spout in the center, the fountain above the bed surface, and the annulus between the spout and the wall, are clearly observed. The solids volume fraction is low in the spout, while the volume fraction is high in the annulus. However, somewhat different fountain heights and spout shapes are obtained for different φ. The fountain heights decrease slightly with the increasing of φ. As shown in Table 3, the fountain height is the highest for $\varphi=0$. When $\varphi=0$, there is no friction between particles and wall, the free slip of particles on the wall results in a higher particles velocity, which consequently leads to a high fountain height. The spout shape for $\varphi=1$, corresponding to a no-slip condition at the wall, shows the greatest deviation from the others. For the no-slip boundary condition, strong friction between particles and wall exists, which resists the downward flow of particles, resulting in a low particle circulation rate. The action region of the entering gas extends because of less particles circulating to the entrance of spouted beds. Hence, the spout diameter near the entrance for $\varphi=1$ is noticeably bigger than other cases.

The specularity coefficient characterizes the friction between particles and wall. A strong friction results in a high wall shear stress. Table 3 compares the wall shear stress at different φ. For $\varphi=0$, there is no friction between the particles and wall, and hence the shear stress is zero. For $\varphi=1$, the particles stick to the wall, and thus the shear stress is the maximum. With increasing φ, the wall shear stress increases significantly. The maximal shear stress reaches to 122 Pa in the present simulation. In spouted beds, the overall pressure drop is balanced by the particles weight and wall shear. The specularity coefficient affects the wall shear stress, consequently, it has an influence on the overall pressure drop. Table 3 compares the pressure drop at different φ. It is clear that the pressure drops predicted at different φ show significant differences. For the free-slip boundary condition, the wall shear stress is zero, and hence the pressure drop is the highest. While for the no-slip condition, the highest wall shear results in the least pressure drop. The significant effect of specularity coefficient

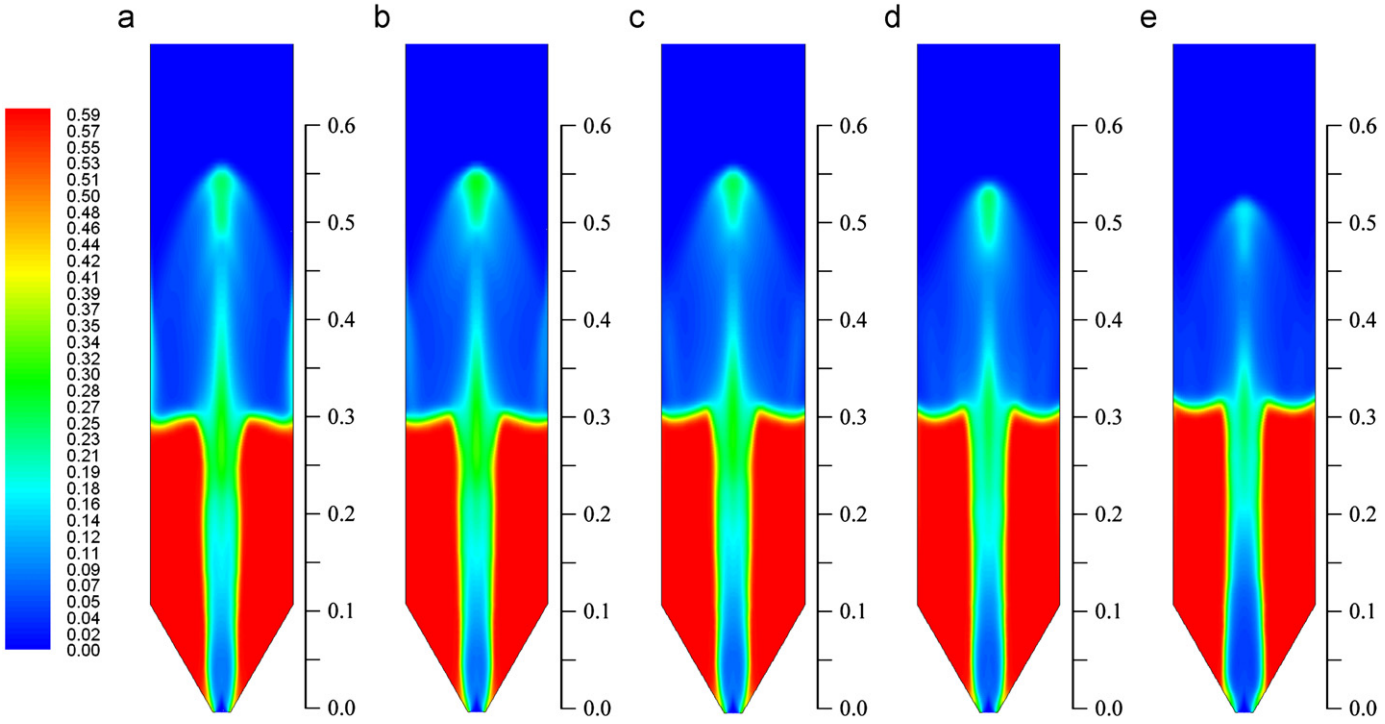

Fig. 4. Predicted solids volume fraction distribution for different specularity coefficients. (a) $\varphi=0$, (b) $\varphi=0.01$, (c) $\varphi=0.05$, (d) $\varphi=0.2$, (e) $\varphi=1$.

Table 3
Fountain heights, wall shear stresses and pressure drops for different specularity coefficients.

Item	Experimental data	Predicted results				
		$\varphi=0$	$\varphi=0.01$	$\varphi=0.05$	$\varphi=0.2$	$\varphi=1$
Fountain height, m	0.25	0.271	0.265	0.259	0.247	0.235
Wall shear stress, Pa	–	0	13	31	53	122
Pressure drop, kPa	3.00	3.45	3.30	3.04	2.77	2.19

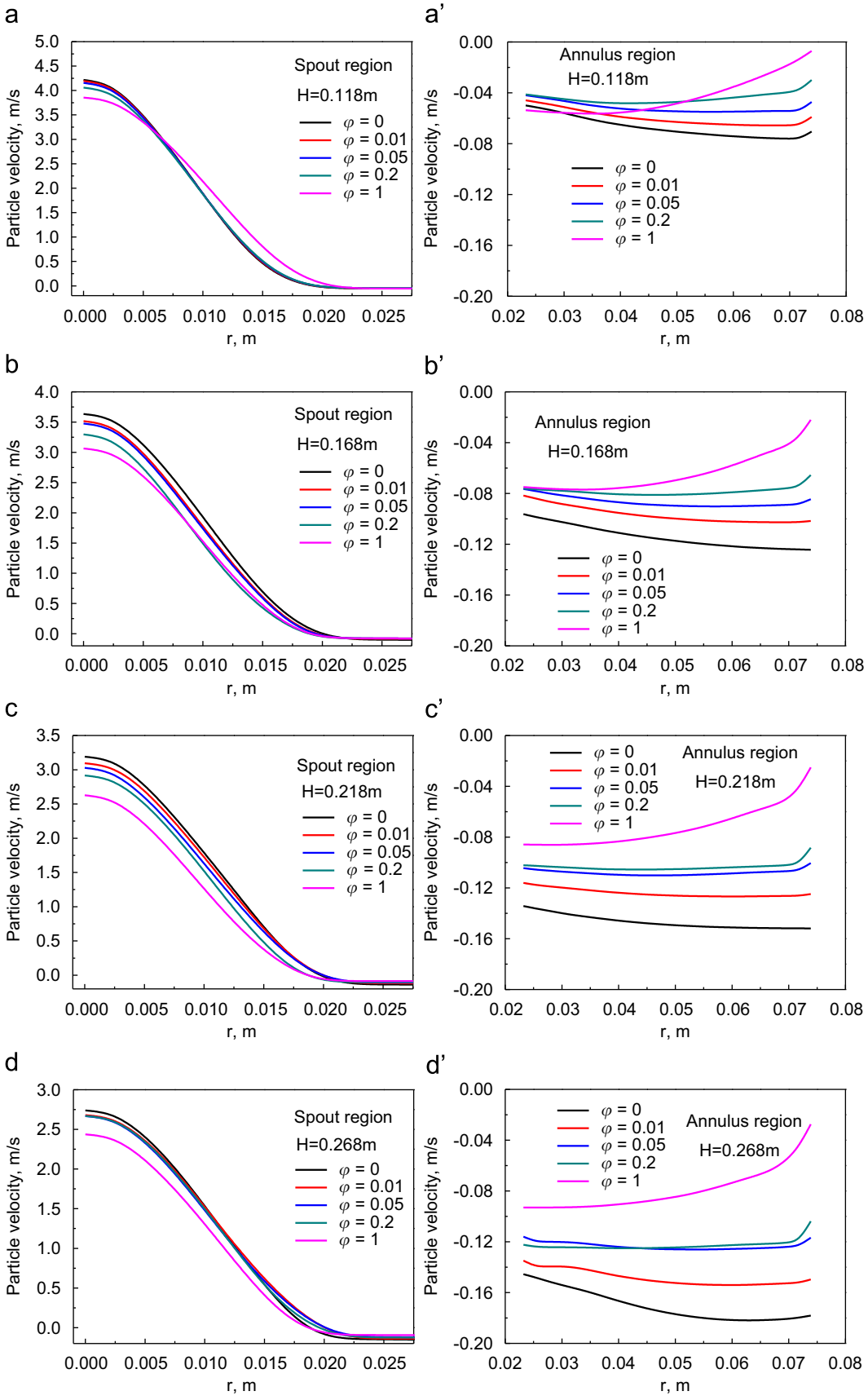

Fig. 5. Radial profiles of particles velocity for different specularity coefficients.

on pressure drop suggests that it is very important to adopt a suitable specularity coefficient for the CFD simulation of spouted beds.

Fig. 5 presents the radial profiles of particles velocity in the spout and annulus region of spouted beds for different specularity coefficients. It is noteworthy that the local particle velocities in the annulus region are negative, indicating that the particles move downwards. There are noticeable differences of particles velocity both in the spout and annulus region for different φ. A smaller specularity coefficient leads to higher particles velocities both in the spout and annulus region. When $\varphi=1$, no-slip boundary condition, the wall shear stress prevents the particles to move downward, resulting in a lower velocity. When $\varphi=0$, the particles can freely slip on the wall and hence the particles have a higher velocity. It can be clearly observed in Fig. 5(a′)–(d′) that there are pronounced difference of particles velocities close to the wall due to the strong effect of friction between particles and wall.

The radial profiles of voidage in the spout region of spouted beds for different specularity coefficients are shown in Fig. 6. The profiles are little different except for $\varphi=1$, which is in accordance with the observation of Fig. 4. Combining all results from Figs. 4, 5 and 6, it is interesting to find that the results for $\varphi=1$ deviate noticeably from the other results for $\varphi=0$, 0.01, 0.05 and 0.2. However, most CFD simulations of spouted beds (Du et al., 2006a, 2006b; Zhonghua and Mujumdar, 2008; Bettega et al., 2009a, 2009c; Duarte et al., 2009; Gryczka et al., 2009; Shuyan et al., 2009, 2010a, 2010b; Dan et al., 2010) used the no-slip ($\varphi=1$) wall boundary conditions for solids phase. Therefore, their simulation results need to be further verified. Accordingly, an appropriate value of specularity coefficient should be obtained by comparing the simulated results with experimental data.

4.3. Effect of particle–wall restitution coefficient

For the numerical simulation of dense gas–solids flows, the particle–wall restitution coefficient, e_w, quantifies the dissipation of solids kinetic energy by collisions with the wall. A value of e_w close to unity implies very low dissipation of granular energy at the wall. The value of 0.8–1 is commonly used. Hence, the influence of the particle–wall restitution coefficient on the flow behavior of spouted beds was evaluated by comparing the simulated results for $e_w=0.8$, 0.9 and 0.99. Fig. 7 shows the simulated solids volume fraction distribution in spouted beds using different e_w. Different particle–wall restitution coefficients give the similar flow pattern. When the fountain heights and pressure drops are compared for different e_w, as shown in Table 4, no pronounced differences are observed.

As shown in Fig. 7, the flow patterns of spouted beds at different e_w are similar. The particle–wall restitution coefficient hardly influences the flow in the spout region. Thus, more interest is focused on the investigation of the flow behavior in annulus region. Fig. 8 shows the predicted granular temperature near the wall for different e_w. The granular temperature rises with increasing e_w. A lower particle–wall restitution coefficient causes more dissipation of the particles fluctuation energy at the wall, leading to the decrease of granular temperature. Similar results were also reported by Natarajan and Hunt (1998). However, for the e_w values tested in the current study, the influence of particle–wall restitution coefficient on the granular temperature profile is fairly minor.

When the particles velocity profiles in the annulus region are examined, as shown in Fig. 9, it is found that varying the wall restitution values does not affect the particles velocities

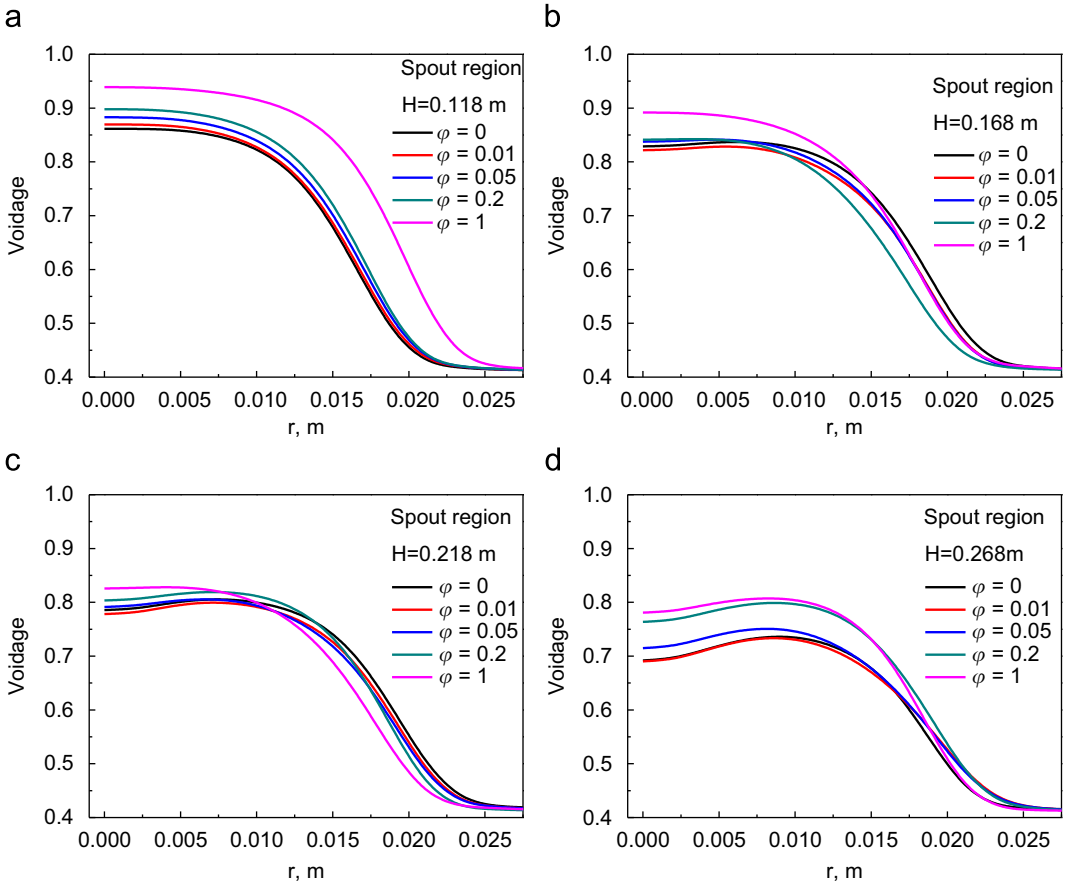

Fig. 6. Radial profiles of voidage in the spout region for different specularity coefficients.

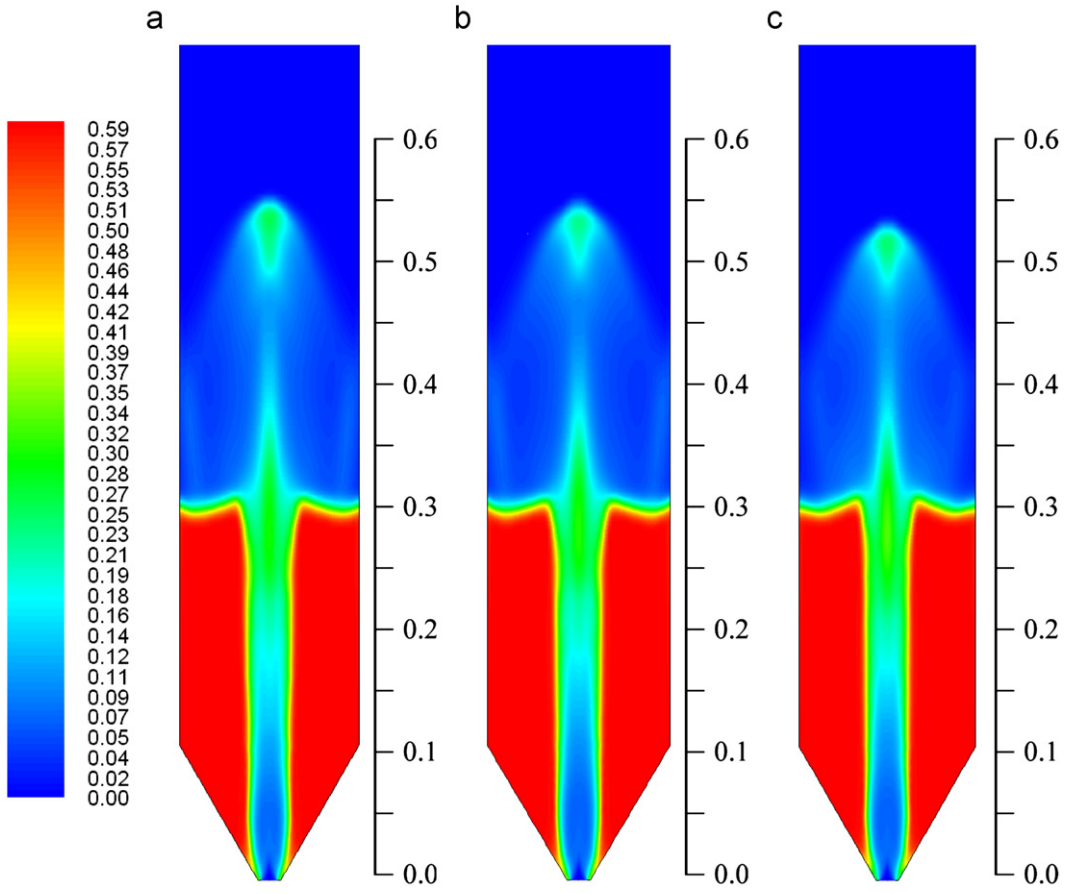

Fig. 7. Predicted solids volume fraction distribution for different particle–wall restitution coefficients. (a) $e_w = 0.8$, (b) $e_w = 0.9$, (c) $e_w = 0.99$.

Table 4
Fountain heights and pressure drops for different particle–wall restitution coefficients.

Item	Experimental data	Predicted results		
		e_w=0.8	e_w=0.9	e_w=0.99
Fountain height, m	0.25	0.259	0.259	0.247
Pressure drop, kPa	3.00	3.07	3.04	3.02

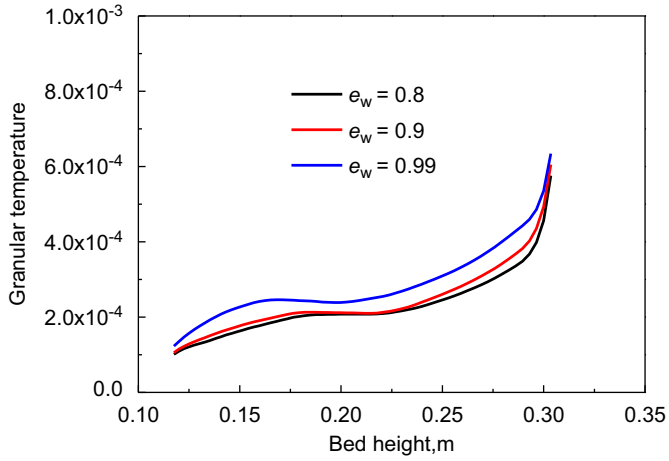

Fig. 8. Predicted granular temperature near the wall for different particle–wall restitution coefficients.

significantly. The differences of particles velocity at different e_w are negligible when compared to the differences at different φ. It can be concluded that the particle–wall restitution coefficient only plays a minor role in the numerical simulation of gas–solids flow in spouted beds. The current results are consistent with the observations by Neri and Gidaspow (2000), McKeen and Pugsley (2003), and Almuttahar and Taghipour (2008). Neri and Gidaspow (2000) examined two wall restitution coefficients of 0.96 and 0.8 for a circulating fluid bed riser, and reported that the wall restitution coefficient had some effect on the solids concentration near the wall, but its value was not critical for the overall definition of the flow pattern.

4.4. Comparison with experimental data

According to the simulation results, the wall boundary condition has a significant effect on the flow behavior of spouted beds, and using a suitable boundary condition is critical for giving proper prediction. However, the parameters of boundary condition are hard to be measured by experiments. Therefore, the simulated results with different wall boundary conditions should be compared with experimental data to determine the suitable parameters. Comparing the predicted fountain heights and pressure drops in Tables 3 and 4, it is clear that the specularity coefficient (φ) has a more pronounced effect on the pressure drop than on the fountain height, while the particle–wall restitution coefficient only plays a small role. The fountain height and bed pressure drop obtained by the experiment of He et al. (1994a, 1994b) was 0.25 m and 3.00 kPa, respectively. These experimental data were used to search for the best value of φ that makes CFD predictions agree

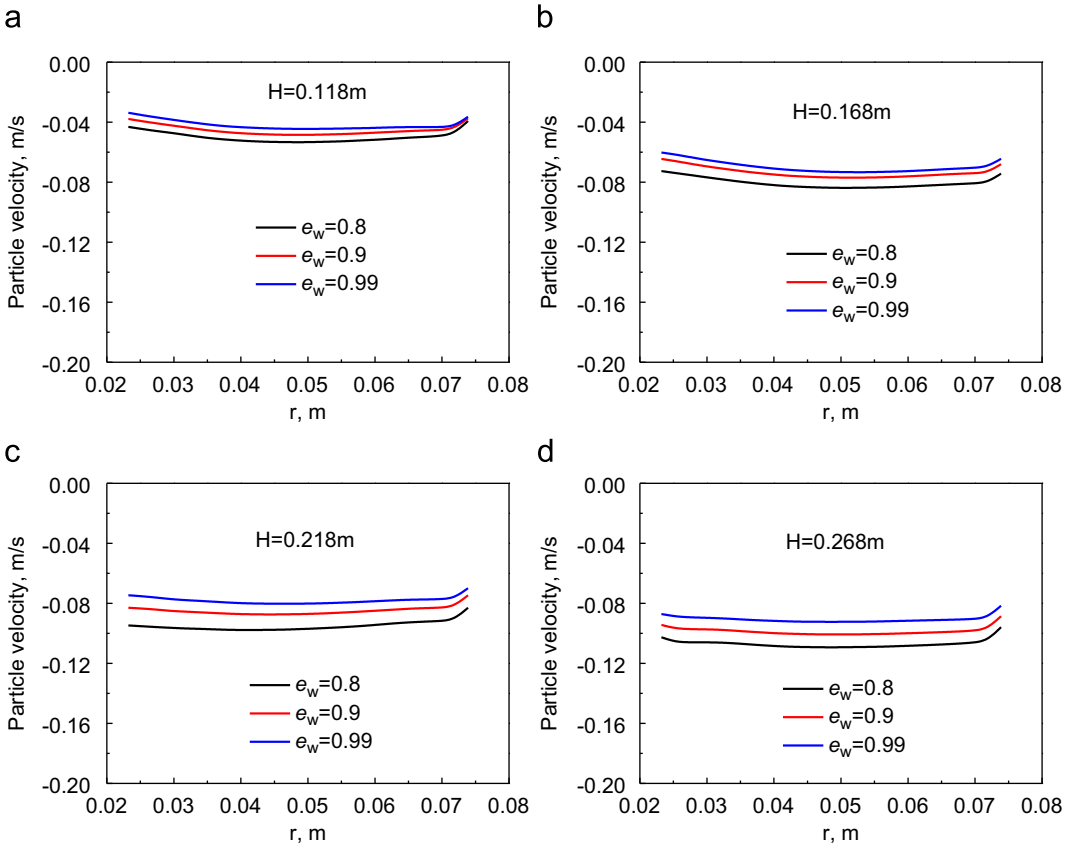

Fig. 9. Radial profiles of particles velocity in the annulus region for different particle–wall restitution coefficients.

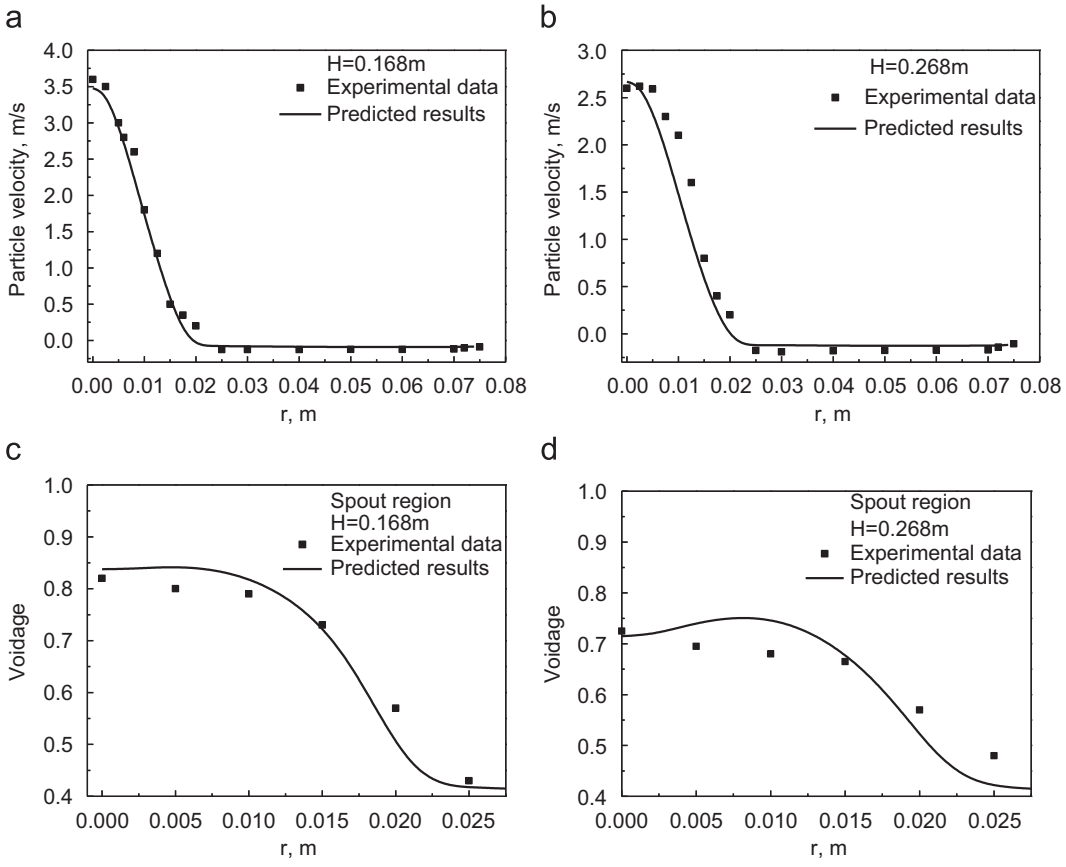

Fig. 10. Comparison of experimental data and predicted results.

with the experiment. Accordingly, comparing the predicted fountain heights and bed pressure drops at different specularity coefficients to the experimental data, the value of $\varphi=0.05$ provides the best agreement with experimental data.

The predicted particles velocity and voidage profiles at $H=0.168$ m and 0.268 m are further compared with experimental measurements, as shown in Fig. 10. The simulated particles velocities are in a good agreement with experimental data, while the voidages are slightly different from those measured. Considering the error produced by the measurement, we think that the deviation is acceptable. Hence, it is suggested that $\varphi=0.05$ is suitable for the CFD modeling of the studied spouted beds. It is noteworthy that there are other parameters used in the CFD models of spouted beds which would affect the validated and suggested values for specularity coefficient and particle–wall restitution coefficient. Hence, this needs uncertainly study and parametric analysis which are beyond the scope of this work. However such analyses are being considered in our future work.

5. Conclusions

TFM approach has been used to investigate the hydrodynamics of spouted beds at different solid-phase wall boundary conditions. Several cases with different specularity coefficients ($\varphi=0$, 0.01, 0.05, 0.2 and 1) and different particle–wall restitution coefficients ($e_w=0.8$, 0.9 and 0.99) were simulated to evaluate their impact on the flow behavior of spouted beds. The spout diameter, fountain height, pressure drop, local voidage and particles velocity obtained from different cases were compared. The simulated results show that the solid-phase wall boundary condition plays an important role in the CFD simulation of spouted beds. The specularity coefficient has a significant effect on the fountain height, wall shear stress, pressure drop and the solids velocity distribution. The particle–wall restitution coefficient plays only a minor role in the modeling of gas–solid flow in spouted beds. The predicted results were compared with the available experimental data in the literature to obtain the suitable values of specularity coefficient and particle–wall restitution coefficient for the CFD simulation of spouted beds.

Nomenclature

$C_\mu, C_{1\varepsilon}, C_{2\varepsilon}$ coefficients in turbulence model
C_D drag coefficient
D_c column diameter, m
D_h hydrodynamic diameter, m
D_i orifice diameter, m
D_s mean spout diameter, m
d_p particle diameter, m
d_s particle diameter, m
e_{ss} particle–particle restitution coefficient
e_w particle–wall restitution coefficient
$G_{k,g}$ production of turbulence kinetic energy
g gravitational constant, m s^{-2}
$g_{0,ss}$ radial distribution function
H static bed height, m
H_F fountain height, m
h bed height, m
I_{2D} the second invariant of the deviatoric stress tensor
$\bar{\bar{I}}$ unit tensor
k_g turbulence quantities of gas phase, m^2 s^{-2}
L column height, m
P pressure, N m^{-2}
P_s solids pressure, N m^{-2}
Re_s particle Reynolds number
T temperature, K
t time, s
U superficial gas velocity, m s^{-1}
v_g gas velocity, m s^{-1}
v_s particles velocity, m s^{-1}
$v_{s,w}$ tangential velocity at the wall, m s^{-1}

Greek letters

α_g gas volume fraction
α_s solids volume fraction
$\alpha_{s,max}$ maximum packing limit of solids
β fluid-particles interaction coefficient, kg m^{-3} s^{-1}
ε_g turbulence dissipation of gas phase, m^2 s^{-3}
ε_o loose packed voidage
ϕ internal friction angle of particle, $^\circ$
ϕ_s particle sphericity
φ specularity coefficient
$\Gamma_{\Theta s}$ diffusion coefficient, J kg^{-1}
$\gamma_{\Theta s}$ energy dissipation, kg m^{-3} s^{-1}
$\bar{\bar{\tau}}_g$ stress tensor for gas phase, N m^{-2}
$\bar{\bar{\tau}}_s$ stress tensor for solids phase, N m^{-2}
λ_s solids bulk viscosity, Pa s
μ_g gas effective viscosity, Pa s
$\mu_{l,g}$ gas molecular viscosity, Pa s
μ_s solids shear viscosity, Pa s
$\mu_{s,col}$ solids collisional viscosity, Pa s
$\mu_{s,fr}$ solids frictional viscosity, Pa s
$\mu_{s,kin}$ solids kinetic viscosity, Pa s
$\mu_{t,g}$ turbulent viscosity, Pa s
$\Pi_{k,g}, \Pi_{\varepsilon,g}$ influence of the dispersed phases on the continuous phase
Θ_s granular temperature, m^2 s^{-2}
Θ_w granular temperature at the wall, m^2 s^{-2}
ρ_f fluid density, kg m^{-3}
ρ_g gas density, kg m^{-3}
ρ_s solid density, kg m^{-3}
$\sigma_k, \sigma_\varepsilon$ Prandtl number

Subscripts

g gas phase
s solid phase

Acknowledgment

The authors acknowledge the financial support by US Department of Energy. Xingying Lan is grateful to the China Scholarship Council and China University of Petroleum (Beijing) for supporting her attachment to Missouri University of Science and Technology, USA.

References

Almuttahar, A., Taghipour, F., 2008. Computational fluid dynamics of high density circulating fluidized bed riser: study of modeling parameters. Powder Technol. 185, 11–23.

Benyahia, S., Syamlal, M., O'Brien, T.J., 2005. Evaluation of boundary conditions used to model dilute, turbulent gas/solids flows in a pipe. Powder Technol. 156, 62–72.

Benyahia, S., Syamlal, M., O'Brien, T.J., 2007. Study of the ability of multiphase continuum models to predict core-annulus flow. AIChE J. 53, 2549–2568.

Bettega, R., Correa, R.G., Freire, J.T., 2009a. Scale-up study of spouted beds using computational fluid dynamics. Can. J. Chem. Eng. 87, 193–203.

Bettega, R., da Rosa, C.A., Correa, R.G., et al., 2009b. Fluid dynamic study of a semicylindrical spouted bed: evaluation of the shear stress effects in the flat wall region using computational fluid dynamics. Ind. Eng. Chem. Res. 48, 11181–11188.

Bettega, R., De Almeida, A.R.F., Correa, R.G., et al., 2009c. CFD modelling of a semi-cylindrical spouted bed: numerical simulation and experimental verification. Can. J. Chem. Eng. 87, 177–184.

Cammarata, L., Lettieri, P., Micale, G.D.M., Colman, D., 2003. 2d and 3d CFD simulations of bubbling fluidized beds using Eulerian–Eulerian models. Int. J. Chem. Reactor Eng., 48–55.

Dan, S., Shuyan, W., Gougdong, L., et al., 2010. Simulations of flow behavior of gas and particles in a spouted bed using a second-order moment method—frictional stresses model. Chem. Eng. Sci. 65, 2635–2648.

Ding, J., Gidaspow, D., 1990. A bubbling fluidization model using kinetic theory of granular flow. AIChE J. 36, 523–538.

Du, W., Bao, X., Xu, J., et al., 2006a. Computational fluid dynamics (CFD) modeling of spouted bed: influence of frictional stress, maximum packing limit and coefficient of restitution of particles. Chem. Eng. Sci. 61, 4558–4570.

Du, W., Bao, X., Xu, J., et al., 2006b. Computational fluid dynamics (CFD) modeling of spouted bed: assessment of drag coefficient correlations. Chem. Eng. Sci. 61, 1401–1420.

Du, W., 2006. Computational Fluid Dynamics (CFD) Modeling and Scaling Up Studies of Spouted Beds. China University of Petroleum, Beijing, China.

Duarte, C.R., Olazar, M., Murata, V.V., et al., 2009. Numerical simulation and experimental study of fluid–particle flows in a spouted bed. Powder Technol. 188, 195–205.

Gidaspow, D., Bezburuah, R., Ding, J., 1992. Hydrodynamics of circulating fluidized beds. Kinetic Theory Approach, Fluidization VII. In: Proceedings of the Seventh Engineering Foundation Conference on Fluidization, pp. 75–82.

Gryczka, O., Heinrich, S., Deen, N.G., et al., 2009. Characterization and CFD-modeling of the hydrodynamics of a prismatic spouted bed apparatus. Chem. Eng. Sci. 64, 3352–3375.

He, Y.L., Lim, C.J., Grace, J.R., et al., 1994a. Measurements of voidage profiles in spouted beds. Can. J. Chem. Eng. 72, 229–234.

He, Y.L., Qin, S.Z., Lim, C.J., et al., 1994b. Particle velocity profiles and solid flow patterns in spouted beds. Can. J. Chem. Eng. 72, 561–568.

Hinze, J.O., 1975. Turbulence. McGraw-Hill, New York.

Huilin, L., Yurong, H., Wentie, L., et al., 2004. Computer simulations of gas–solid flow in spouted beds using kinetic–frictional stress model of granular flow. Chem. Eng. Sci. 59, 865–878.

Johnson, P.C., Jackson, R., 1987. Frictional–collisional constitutive relations for granular materials, with application to plane shearing. J. Fluid Mech. 176, 67–93.

Li, T., Grace, J., Bi, X., 2010a. Study of wall boundary condition in numerical simulations of bubbling fluidized beds. Powder Technol. 203, 447–457.

Li, T., Zhang, Y., Grace, J.R., et al., 2010b. Numerical investigation of gas mixing in gas–solid fluidized beds. AIChE J. 56, 2280–2296.

Lun, C.K., Savage, S.B., Jeffrey, D.J., Chepurniy, N., 1984. Kinetic theories for granular flow: inelastic particles in Couette flow and slightly inelastic particles in general flow field. J. Fluid Mech. 140, 223–256.

Mathur, K.B., Epstein, N., 1974. Spouted Beds. Academic Press, New York.

McKeen, T., Pugsley, T., 2003. Simulation and experimental validation of a freely bubbling bed of FCC catalyst. Powder Technol. 129, 139–152.

Natarajan, V.V.R., Hunt, M.L., 1998. Kinetic theory analysis of heat transfer in granular flows. Int. J. Heat Mass Transfer 41, 1929–1944.

Neri, A., Gidaspow, D., 2000. Riser hydrodynamics: simulation using kinetic theory. AIChE J. 46, 52–67.

Peirano, E., Delloume, V., Leckner, B., 2001. Two- or three-dimensional simulations of turbulent gas–solid flows applied to fluidization. Chem. Eng. Sci. 56, 4787–4799.

Schaeffer, D.G., 1987. Instability in the evolution equations describing incompressible granular flow. J. Differential Equations 66, 19–50.

Shuyan, W., Xiang, L., Huilin, L., et al., 2009. Numerical simulations of flow behavior of gas and particles in spouted beds using frictional–kinetic stresses model. Powder Technol. 196, 184–193.

Shuyan, W., Yongjian, L., Yikun, L., et al., 2010a. Simulations of flow behavior of gas and particles in spouted bed with a porous draft tube. Powder Technol. 199, 238–247.

Shuyan, W., Zhenghua, H., Dan, S., et al., 2010b. Hydrodynamic simulations of gas-solid spouted bed with a draft tube. Chem. Eng. Sci. 65, 1322–1333.

Wang, X., Jin, B., Zhong, W., et al., 2009. Modeling on the hydrodynamics of a high-flux circulating fluidized bed with Geldart Group A particles by kinetic theory of granular flow. Energy Fuels 24, 1242–1259.

Wang, Z.G., Bi, H.T., Lim, C.J., 2006. Numerical simulations of hydrodynamic behaviors in conical spouted beds. China Particuol. 4, 194–203.

Zhang, S.J., Yu, A.B., 2002. Computational investigation of slugging behaviour in gas-fluidised beds. Powder Technol. 123, 147–165.

Zhonghua, W., Mujumdar, A.S., 2008. CFD modeling of the gas–particle flow behavior in spouted beds. Powder Technol. 183, 260–272.